

Michail N. Taran · Monika Koch-Müller · Klaus Langer

## Electronic absorption spectroscopy of natural (Fe<sup>2+</sup>, Fe<sup>3+</sup>)-bearing spinels of spinel s.s.-hercynite and gahnite-hercynite solid solutions at different temperatures and high-pressures

Received: 25 May 2004 / Accepted: 26 January 2005 / Published online: 20 May 2005  
© Springer-Verlag 2005

**Abstract** Natural Fe<sup>2+</sup>, Fe<sup>3+</sup>-bearing spinel solid solutions from the spinel s.s.-hercynite and gahnite-hercynite series were analyzed and studied by electronic absorption spectroscopy in the spectral range 30000–3500 cm<sup>-1</sup> in the temperature and pressure ranges 77 ≤ T<sub>K</sub> ≤ 600 and 10<sup>-4</sup> ≤ P<sub>GPa</sub> ≤ 11.0. Two crystals were light-violet in color (type I) and six green or bluish-green (type II). The spectra of both types of spinels are dominated by an UV-absorption edge near 28000 to 24000 cm<sup>-1</sup>, depending on the iron contents, and a very intense band system in the NIR centered around 5000 cm<sup>-1</sup>, which is caused by spin-allowed *dd*-transition of tetrahedral Fe<sup>2+</sup>, derived from <sup>5</sup>E → <sup>5</sup>T<sub>2</sub>. The strong band is in all spinels studied, split into four sub-bands, which can only be observed in very thin platelets. Between the UV-edge and the high-energy wing of the NIR-band there occur a number of very weak bands in type I spinels while the green type II spinels show some of these with significantly enhanced intensity. The intensity of the very weak bands is nearly independent from temperature. Such bands are attributed to spin-forbidden electronic transitions of <sup>IV</sup>Fe<sup>2+</sup>. Temperature and pressure dependence of the intensity enhanced bands of spinels type II indicate that they are caused by <sup>IV</sup>Fe<sup>2+</sup> and <sup>VI</sup>Fe<sup>3+</sup>.

They are attributed to spin-forbidden transitions <sup>6</sup>A<sub>1g</sub> → <sup>4</sup>A<sub>1g</sub>, <sup>4</sup>E<sub>g</sub> → <sup>4</sup>T<sub>2g</sub> and → <sup>4</sup>T<sub>1g</sub> of <sup>VI</sup>Fe<sup>3+</sup>, the two latter being strongly intensified by exchange-coupling interaction with adjacent <sup>IV</sup>Fe<sup>2+</sup>. The pressure dependence of <sup>IV</sup>Fe<sup>2+</sup> *dd*-band system in the NIR caused by spin-allowed <sup>5</sup>E → <sup>5</sup>T<sub>2</sub> transition noticeably differs from that of octahedral Fe<sup>2+</sup>, an effect which is attributed to a dynamic Jahn-Teller effect of <sup>IV</sup>Fe<sup>2+</sup> in the spinel structure.

**Keywords** Electronic spectra · Low and high temperature · High pressure · Spinel · 3d-ions · Exchange-coupling interaction · Jahn-Teller effect

### Introduction

Most minerals of the spinel group have the general formula <sup>IV</sup>(A<sub>1-δ</sub>B<sub>δ</sub>)<sup>VI</sup>(A<sub>δ</sub>B<sub>2-δ</sub>)O<sub>4</sub>. A and B are di- and trivalent cations, respectively, of appropriate size as Mg, Fe<sup>2+</sup>, Zn and Mn<sup>2+</sup> or Al, Fe<sup>3+</sup> and Cr, respectively. δ is called the inversion parameter: when δ = 0 then tetrahedral sites contain divalent cations A<sup>2+</sup> only and the mineral is called normal-spinel (e.g. spinel s.s., hercynite). When δ = 1 the spinel is called inverse with the tetrahedral sites containing exclusively B<sup>3+</sup> (magnetite, magnesioferrite). Such strongly ordered spinels are typical for low temperature origin, whereas with increasing temperature cation disorder increases for both types of spinels. The structure is cubic, space group Fd3m, Z = 8. It is based on a fcc arrangement of oxygen, wherein 1/2 of the octahedral and 1/8 of tetrahedral voids are occupied by the cations in a strictly ordered manner such that the octahedra are edge connected to form strait chains parallel to [110], whereas the tetrahedra are connected by their corners to the octahedral chains. This pattern enables with certain cations A and B and at certain inversion parameters δ strong charge-transfer processes and electronic exchange coupling, such that the respective spinel-minerals are opaque, e.g. magnetite,

M. N. Taran (✉)  
Institute of Geochemistry,  
Mineralogy and Ore Formation,  
National Academy of Science of Ukraine,  
Palladin Ave., 34, 03680 Kyiv-142, Ukraine  
E-mail: taran@igmr.relc.com  
Tel.: +38-0444241270  
Fax: +38-0444240043

M. Koch-Müller  
Sektion 4.1, GeoForschungsZentrum,  
Telegrafenberg, 14473 Potsdam, Germany  
E-mail: mkoch@gfz-potsdam.de  
Tel.: +49-331-288-1492/1402  
Fax: +49-331-288-1492/1402

K. Langer  
Institute of Applied Geosciences,  
Technical University of Berlin,  
10623 Berlin, Germany

${}^{\text{IV}}\text{Fe}^{3+} {}_2(\text{Fe}^{2+} \text{Fe}^{3+})\text{O}_4$ , or chromite  ${}^{\text{IV}}\text{Fe}^{2+} \text{Cr}_2\text{O}_4$ . Despite the many studies by electronic absorption spectroscopy of non-opaque spinel minerals (cf. Burns 1993), not all spectral properties are unambiguously interpreted and evaluated.

In recent publications of Andreozzi et al. (2001) and Hålenius et al. (2002) on electronic absorption spectra of synthetic spinels of spinel sensu stricto (s.s.)-magnesioferrite and spinel s.s.-hercynite compositions, the importance of  ${}^{\text{IV}}\text{Fe}^{3+}$  and  ${}^{\text{VI}}\text{Fe}^{2+}$  was established. These authors attributed the intense and relatively narrow band at  $21300 \text{ cm}^{-1}$  in spectra of spinel s.s.-magnesioferrite spinels to electronic transition  ${}^6A_1 \rightarrow {}^4A_1, {}^4E$  of exchange-coupled pair (ECP)  ${}^{\text{IV}}\text{Fe}^{3+} - {}^{\text{VI}}\text{Fe}^{3+}$ , and two broad bands at  $14500 \text{ cm}^{-1}$  and  $\sim 9500 \text{ cm}^{-1}$  in spinel s.s.-hercynites to electronic intervalence charge-transfer transition (IVCT)  ${}^{\text{VI}}\text{Fe}^{2+} + {}^{\text{VI}}\text{Fe}^{3+} \rightarrow {}^{\text{VI}}\text{Fe}^{3+} + {}^{\text{VI}}\text{Fe}^{2+}$  and spin-allowed transition  ${}^5T_{2g} \rightarrow {}^5E_g$  of  ${}^{\text{VI}}\text{Fe}^{2+}$  enhanced by exchange-coupling interaction with neighboring  ${}^{\text{VI}}\text{Fe}^{3+}$  ion, respectively. However, the absorption spectra of natural spinels of similar compositions emphatically differ from those of synthetic spinels. The reason of this observation is most probably the higher degree of disorder in the synthetic spinels compared to natural ones. Particularly, in natural spinels no IVCT, but exchange-coupled pairs of iron ions is assumed to play an important role in electronic spectra and coloration (Taran et al. 1987). Such more or less hypothetical conclusions can be ascertained in the following way: it is known that the response of absorption bands in electronic spectra of  $\text{Fe}^{2+}$ ,  $\text{Fe}^{3+}$ -bearing minerals on temperature or pressure may give information for their attribution to various types of electronic transitions (Smith and Strens 1976, Smith 1977, Taran et al. 1996, Taran and Langer 1998). Therefore, we studied spectra of natural iron-bearing spinels of predominantly spinel s.s. and gahnite compositions with various, up to  $\sim 30$  mol.%, hercynite component, at different temperatures and pressures. The focus of our study was to elucidate the origin of electronic absorption bands in these spinels in respect to the presence of  $\text{Fe}^{2+} + \text{Fe}^{3+} \rightarrow \text{Fe}^{3+} + \text{Fe}^{2+}$  IVCT and  $\text{Fe}^{2+} \text{Fe}^{3+}$  ECP. Also, it was interesting to investigate a pressure effect on spin-allowed bands of  ${}^{\text{IV}}\text{Fe}^{2+}$  undergone to a dynamic Jahn-Teller effect (e.g. Taran and Langer 2001, Skogby and Hålenius 2003).

## Experimental Details

### Chemical composition of samples

Eight spinels from two provinces were available for investigations. Four samples come from the Pamir region (Tadjikistan) and four from carbonatite rocks of the Ukrainian shield. Chemical analyses of seven spinels, designated as Sp#1 to Sp#7, were determined with a Cameca SX100 electron microprobe using rhodonite (Mn),  $\text{Fe}_2\text{O}_3$  (Fe), NiO (Ni), gahnite (Zn), CoO (Co),

rutile (Ti), wollastonite (Ca, Si), chromite (Cr), olivine (Mg) and  $\text{Al}_2\text{O}_3$  (Al) as standards. Spinel Sp#8, a small,  $\sim 0.5$  mm, crystal fragment, has been selected from sample no. 18500 of carbonatite rocks of the Ukrainian shield (Siroshstan et al. 1976). Averaged over many grains, the crystal-chemical formula of this sample calculated from wet chemical analysis, was taken from Siroshstan et al. (1976).

### Sample preparation for electronic absorption spectroscopy

The samples for optical spectroscopy study at ambient pressure were prepared as polished self-supporting plates of thickness, depending on intensity of absorption bands in the visible and NIR range, from ca 0.1 to 3 mm. The thicknesses were measured with a micrometric screw. Inspection under an optical microscope shows that the plates are homogeneously colored, nearly perfectly transparent; some of them contain inclusions, cracks and other imperfections. Zones free of such imperfections were chosen for spectroscopic measurements.

### Spectroscopic methods

Electronic absorption spectra were recorded in the range ca.  $28500\text{--}6000 \text{ cm}^{-1}$  with a single-beam microspectrophotometer, which consists of a SpectraPro-275 triple grating monochromator connected to a highly modified MIN-8 polarizing microscope and controlled by PC. The spectra were scanned with steps  $\Delta\lambda = 1$  nm in the range 350–450 nm (ca.  $28500\text{--}22222 \text{ cm}^{-1}$ ),  $\Delta\lambda = 2$  nm in the range 420–1000 nm ( $\sim 22222\text{--}10000 \text{ cm}^{-1}$ ) and  $\Delta\lambda = 5$  nm in the range 1000–1650 nm ( $10000\text{--}ca. 6060 \text{ cm}^{-1}$ ).

Spectra at liquid nitrogen temperature ( $\sim 77$  K) were measured using a home-made miniature cryostat attached to the microscope stage. To maintain good thermal contact the samples were placed on a transparent supporting plate prepared from synthetic high-quality single-crystal sapphire (see e.g. Volkov et al. 1981). Besides, they were glued to the supporting plate and the latter to the cooled sample holder with vacuum grease. The cryostat was evacuated to pressure  $\sim 10^{-5}$  torr, low enough to prevent any moisture condensation on the external surfaces of the cryostat windows.

A miniature electric furnace with an electronic control device, providing temperature stability  $\pm 5$  K, to register spectra at temperatures from 300 K to 600 K, was attached to the spectrophotometer.

High pressure spectroscopic measurements in the UV-VIS-NIR were accomplished on polished plates of ca. 30  $\mu\text{m}$  thick prepared from three high-iron samples, Sp#5, #6 and #8. High-pressure spectra in the NIR range 7000 to  $3000 \text{ cm}^{-1}$  were obtained on two spinels of different iron contents, Sp#1 and #6. To generate

hydrostatic pressure up to  $\sim 10$  GPa, the diamond anvils cell (DAC) techniques were used as described elsewhere (e.g. Langer et al. 1997).

Room temperature and in-situ high-pressure NIR spectra (up to  $\sim 10$  GPa) in the range  $7500\text{--}3000\text{ cm}^{-1}$  were recorded on a Bruker ISF 66v FTIR spectrometer. The spectrometer was equipped with a ceramic light source, a KBr beam-splitter and a Hyperion microscope using Cassegrainian objectives and an InSb detector. The spectra were taken with an aperture size of  $100\times 50\text{ }\mu\text{m}$  and a resolution of  $2\text{ cm}^{-1}$ . For each spot the spectrum was averaged for 128 scans. Polished spinel platelet, about  $120\times 180\times 40\text{ }\mu\text{m}$  in size, and ruby chips were embedded in the gasket hole (diameter of  $300\text{ }\mu\text{m}$ ) with CsI as a pressure medium. There were four stages of pressure application. First, the spectra were scanned at pressures stepwise increasing from the ambient one to 10 GPa. In the second stage pressure was released and decreases to ambient conditions. At the third stage, pressure was increased again to 10.7 GPa and finally at the fourth stage released to ambient pressure.

Spectra were fitted with Gaussian components using Jandel Scientific software Peakfit 4.0. Choice of a shape of the high-energy absorption edge, overlapping UV and a part of the visible range of the spectra, was the biggest problem of the procedure, especially in cases of type II spinels (see below), wherein the edge is extremely strong. This uncertainty is the main disadvantage of the procedure frequently resulting in unexpected differences in energies, intensities and widths of component Gaussian bands in spectra of different samples. This is especially true for relatively weak components which characteristics may vary very significantly. By our experience the absorption edge is to be best fitted by a sum of Gaussian and Lorentz curves.

## Results

Crystal chemical formulae of the spinels studied, calculated from microprobe and wet chemical analyses, are given in Table 1. The calculations are based on the

**Table 1** Spinel crystals studied: Type I or type II spinels are light-violet or green and bluish-green, respectively. Microprobe analyses are recalculated in terms of crystallochemical formulae. Uncertainties of at. pfu is in the last decimal point.  $\text{Fe}^{2+}$  and  $\text{Fe}^{3+}$  are

Spinel#	Type	Source	Composition
1	I	Pamir <sup>a)</sup>	$\text{IV}(\text{Mg}_{0.980}\text{Fe}^{2+}_{0.020})_{\Sigma 1.000}\text{VI}(\text{Al}_{1.992}\text{Fe}^{3+}_{0.010})_{\Sigma 2.002}\text{O}_4$
2	I	Ukraine <sup>b)</sup>	$\text{IV}(\text{Zn}_{0.001}\text{Mg}_{0.942}\text{Fe}^{2+}_{0.057})_{\Sigma 1.000}\text{VI}(\text{Al}_{1.986}\text{Fe}^{3+}_{0.011}\text{Cr}_{0.002})_{\Sigma 1.999}\text{O}_4$
3	II	Pamir	$\text{IV}(\text{Zn}_{0.738}\text{Mg}_{0.010}\text{Fe}^{2+}_{0.252})_{\Sigma 1.000}\text{VI}(\text{Al}_{1.995}\text{Fe}^{3+}_{0.003}\text{Cr}_{0.003})_{\Sigma 2.001}\text{O}_4$
4	II	Pamir	$\text{IV}(\text{Zn}_{0.694}\text{Mg}_{0.013}\text{Fe}^{2+}_{0.291}\text{Co}_{0.001})_{\Sigma 1.000}\text{VI}(\text{Al}_{1.989}\text{Fe}^{3+}_{0.007}\text{Cr}_{0.002})_{\Sigma 1.998}\text{O}_4$
5	II	Pamir	$\text{IV}(\text{Zn}_{0.805}\text{Mg}_{0.021}\text{Fe}^{2+}_{0.172})_{\Sigma 0.998}\text{VI}(\text{Al}_{1.983}\text{Fe}^{3+}_{0.017})_{\Sigma 2.000}\text{O}_4$
6	II	Ukraine <sup>b)</sup>	$\text{IV}(\text{Zn}_{0.009}\text{Mg}_{0.854}\text{Fe}^{2+}_{0.136})_{\Sigma 0.999}\text{VI}(\text{Al}_{1.979}\text{Fe}^{3+}_{0.019})_{\Sigma 1.998}\text{O}_4$
7	II	Ukraine <sup>b)</sup>	$\text{IV}(\text{Zn}_{0.008}\text{Mg}_{0.964}\text{Fe}^{2+}_{0.026})_{\Sigma 0.998}\text{VI}(\text{Al}_{1.982}\text{Fe}^{3+}_{0.017}\text{Cr}_{0.001})_{\Sigma 2.000}\text{O}_4$
8	II	Ukraine <sup>c)</sup>	$\text{IV}(\text{Mg}_{0.78}\text{Fe}^{2+}_{0.13}\text{Mn}_{0.01})_{\Sigma 0.92}\text{VI}(\text{Al}_{1.98}\text{Fe}^{3+}_{0.1})_{\Sigma 1.99}\text{O}_{4.04}$

<sup>a)</sup> Litsarev et al. (1980); <sup>b)</sup> Taran et al. (1988); <sup>c)</sup> Siroshtan et al. (1976). In all samples from #1 to 7 some minor amounts of Si, Ca, Mn, Ni and Co (from 0.000 n to 0.00 n wt.%), that is near the lowest limit of microprobe analysis, were also detected.

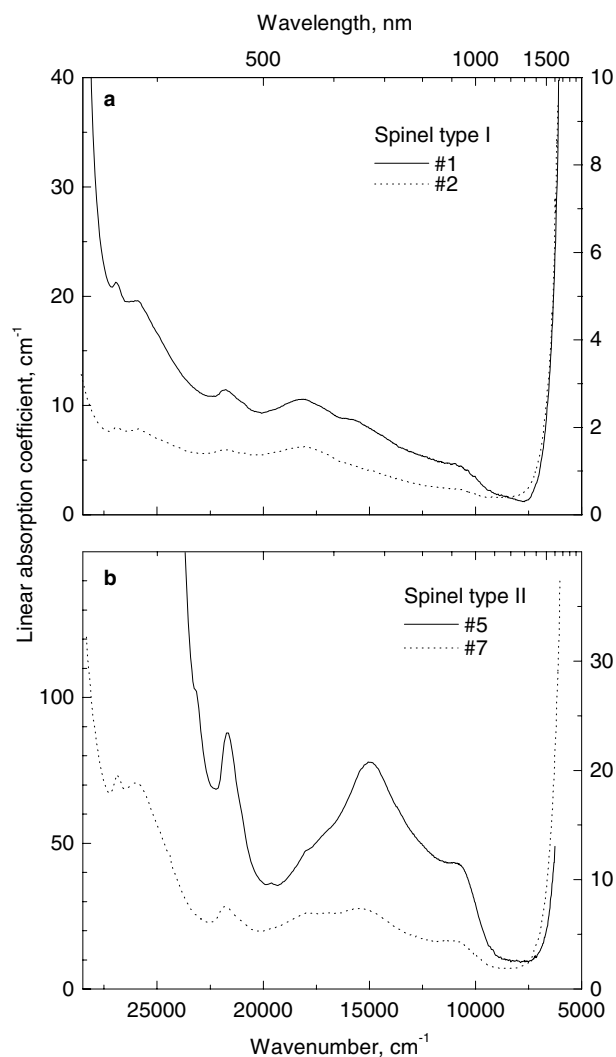


**Fig. 1** Typical spectra of light-violet spinels type I, #1 and #2 (Table 1), and green spinels type II, #5 and #7 (Table 1), at ambient conditions. The linear absorption coefficient values,  $\alpha[\text{cm}^{-1}]$ , of the solid and dotted spectra are shown on the left and right ordinate axes, respectively

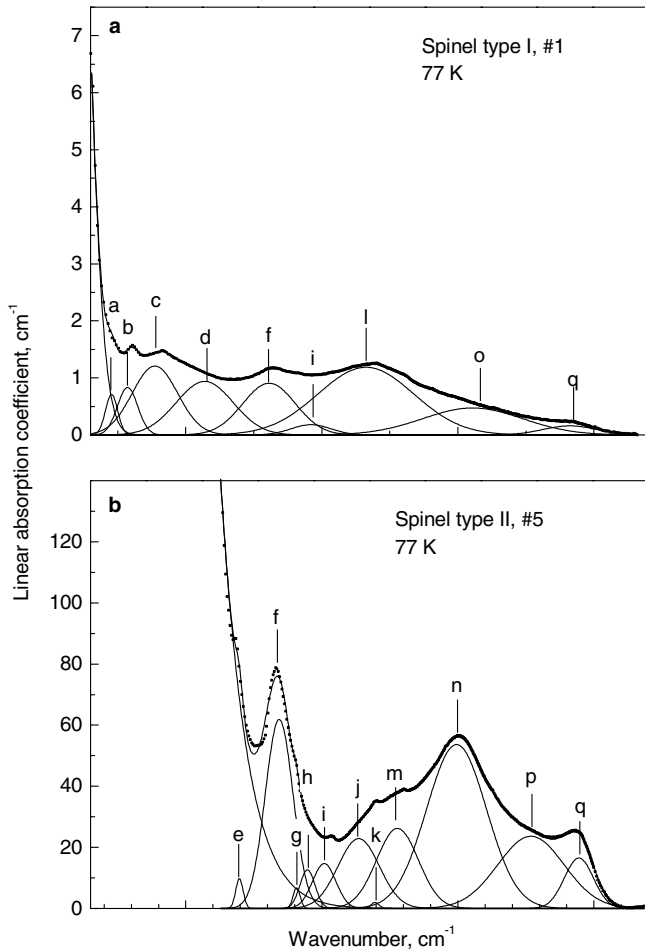


**Fig. 2** Curve resolved spectra of type I spinel #1 and type II spinel #5 in the spectral range 28500–8000  $\text{cm}^{-1}$ . The spectra were measured at 77 K

assumption of predominantly normal distribution of  $\text{Fe}^{2+}$  and  $\text{Fe}^{3+}$  which is usual for spinels of s.s.-hercynite and gahnite-hercynite compositions of relative low temperature origin. Of course, on the basis of microprobe composition only we can not be sure about the real  $\text{Fe}^{2+}$ - and  $\text{Fe}^{3+}$ -distribution in the samples and very small amounts of  $^{IV}\text{Fe}^{3+}$  and  $^{VI}\text{Fe}^{2+}$  may exist. However, such small concentrations are hardly detectable by Mössbauer spectroscopy. As seen from Table 1, iron, presumably as  $^{IV}\text{Fe}^{2+}$  and  $^{VI}\text{Fe}^{3+}$ , is a major transition metal component in all of them and, therefore, we assume that most features in absorption spectra of the samples are caused by these iron ions.

Three samples from Pamir (Sp#3 – Sp#5) are of high Zn-contents thus belonging predominantly to the gahnite-hercynite series. All other samples are mostly of spinel s.s. – hercynite compositions.

By color and absorption spectra the spinels studied may be divided to two groups, I and II. The group I is represented by two samples, Sp#1 and #2, of light violet color. Sp#3-Sp#8, assigned to group II, are of green and bluish-green colors.

**Table 2** Results of curve fitting in the energy range 28,000–10,000  $\text{cm}^{-1}$  of the spectra of spinel type I, #1, and II, #5, at 77 and 300 K (cf. Fig. 2). FWHM = full band width at half maximum height

Band	Spinel#1, 77 K			Spinel#5, 77 K			Spinel#5, 300 K					
	Energy, $\text{cm}^{-1}$	Linear intensity, $\text{cm}^{-1}$	Integral intensity, $\text{cm}^{-2}$	Band width HWHM, $\text{cm}^{-1}$	Energy, $\text{cm}^{-1}$	Linear intensity, $\text{cm}^{-1}$	Integral intensity, $\text{cm}^{-2}$	Band width HWHM, $\text{cm}^{-1}$	Energy, $\text{cm}^{-1}$	Linear intensity, $\text{cm}^{-1}$	Integral intensity, $\text{cm}^{-2}$	Band width HWHM, $\text{cm}^{-1}$
a	27730	0.71	400	530	23030	9.75	3310	320	22960	8.30	3210	360
b	27140	0.83	780	880	21570	61.94	79123	1200	21560	53.46	72770	1280
c	26130	1.21	2520	1963	20930	6.76	2180	300	20930	5.90	2690	430
d	24305	0.94	2460	2465	20530	12.66	8770	650	20500	13.13	10200	730
e	21940	0.91	2200	2278	19910	14.69	15790	1010	19870	16.90	20650	1150
f	20400	0.18	330	1715	18650	22.87	43490	1790	18650	25.04	53880	2020
g					18040	1.98	720	340	17960	0.62	195	290
h					17220	26.20	50550	1810	17180	28.30	67140	2230
i					15050	53.63	148140	2590	15040	59.73	181750	2860
j					12310	23.62	72150	2870	12420	31.05	109330	3310
k					10550	16.51	22070	1260	10580	16.32	28200	1620
l	18380	1.19	5230	4140								
m												
n	14460	0.47	2170	4310								
o												
p	10890	0.16	390	2310								
q												

This energy range is overlapped by the low-energy wing of the UV absorption bands

Typical spectra of spinels of the two types, I and II, are shown in Fig. 1, a and b, respectively. As seen from the Figure, in both cases spectra consist of the high- and low-energy absorption edges, which form a “transparent window” in the visible and, partly, in the adjacent UV and NIR ranges. Note that the low-energy edge is undoubtedly a wing of the spin-allowed band system, derived from electronic  ${}^5E \rightarrow {}^5T_2$  transition of  ${}^{IV}\text{Fe}^{2+}$ , which is extremely strong in natural Fe-bearing spinels (e.g. Burns 1993, Rossman and Taran 2001, Taran and Langer 2001).

Within the “windows” there is a series of absorption bands superimposed on the high-energy edge, which are distinctly different by their number, shape and, especially, intensity in the spectra of spinels of the group I and II.

The results of the curve-fitting of the spectra of Sp#1 (77 K), type I, and Sp#5 (77 and 300 K), type II, are shown in Fig. 2 and Table 2. At least nine Gaussians are necessary for a satisfactory fit of Sp#1, type I (Fig. 2a). In case on Sp#5, type II, as many as eleven Gaussian bands are necessary for the fit (Fig. 2b). Note that in both cases most of the component Gaussians are perceivable in the original spectra.

For clearness we took a common labeling of the component bands in spectra of Sp#1 and #5, *a* to *q*, assuming that in Sp#5 the UV bands *a* to *d* when they occur in this type II spinel, are hidden under the strong high-energy edge shifted to the visible range (Fig. 2, Table 2). Note in this respect that *b*- and *c*-bands are distinct in the spectrum of relatively low-iron Sp#7, type II (Fig. 1b).

It is remarkable that in spectra of spinels of type II ratio of intensities of the bands designated as *n*, *p* and *q*, remains nearly constant from sample to sample. This suggests that these three bands originate from a common center. Relative intensities of all other bands are variant from sample to sample.

Energies of all *e*- to *q*-bands in spectra of all spinels type II studied do not noticeably depend on iron content, but slightly depend on zinc concentration. Thus, in Sp#6 and #7 of nearly equal Zn-, but of significantly different Fe-contents (Table 1) energies of the most prominent bands *f*, *n* and *q*, practically do not vary. On the other hand, in Zn-enriched Sp#3-Sp#5 the energies of *n*- and *q*-bands are noticeably lower ( $\sim 500$  and  $\sim 200$   $\text{cm}^{-1}$ , respectively) than in Sp#6 and #7, whereas that of *f*-band remains practically the same.

Spectra of Sp#1, type I, and #5, type II, measured at different temperatures from 77 to 600 K, are shown in Fig. 3, a and b, respectively. In both samples increase of temperature causes shift of the high-energy edge to lower energies. On the contrary, the high-energy wing of the spin-allowed bands of  ${}^{IV}\text{Fe}^{2+}$  displays a distinct “blue” shift. As seen from the Fig. 3a and as derived by curve fitting analyses, at increasing temperature all bands in spectrum of Sp#1, type I, become weaker and broader whilst their energies remain nearly unchanged. In the contrary, in Sp#5, type II, in the temperature range from

77 to 300 K there takes place a remarkable enhancement of integral intensities of all bands, except *f* (Table 2). Note that bands *k*, *g* and *e* are relatively weak (Fig. 2, Table 2), therefore, their characteristics obtained by the curve resolution are not very reliable. At temperatures higher than ca. 300 K (up to 600 K) integral intensities of the bands in spectrum of Sp#5 remain nearly unchanged: the bands only become broader and, thus, less resolved (Fig. 3b). Curve fitting could not reveal any regular change of the band’s energies with temperature. Only for the most intense *n*-band a slight shift to higher energies, from  $\sim 15050$   $\text{cm}^{-1}$  at 77 K to  $\sim 15330$   $\text{cm}^{-1}$  at 600 K, was detected.

Spectroscopic study of three spinels, Sp#5, #6 and #8, type II, at different pressures (Fig. 4, a, b and c, respectively) give rather convergent results. In all samples the increasing pressure causes a regular shift of the wing of  ${}^5E \rightarrow {}^5T_2$  band of  ${}^{IV}\text{Fe}^{2+}$  to higher energies,

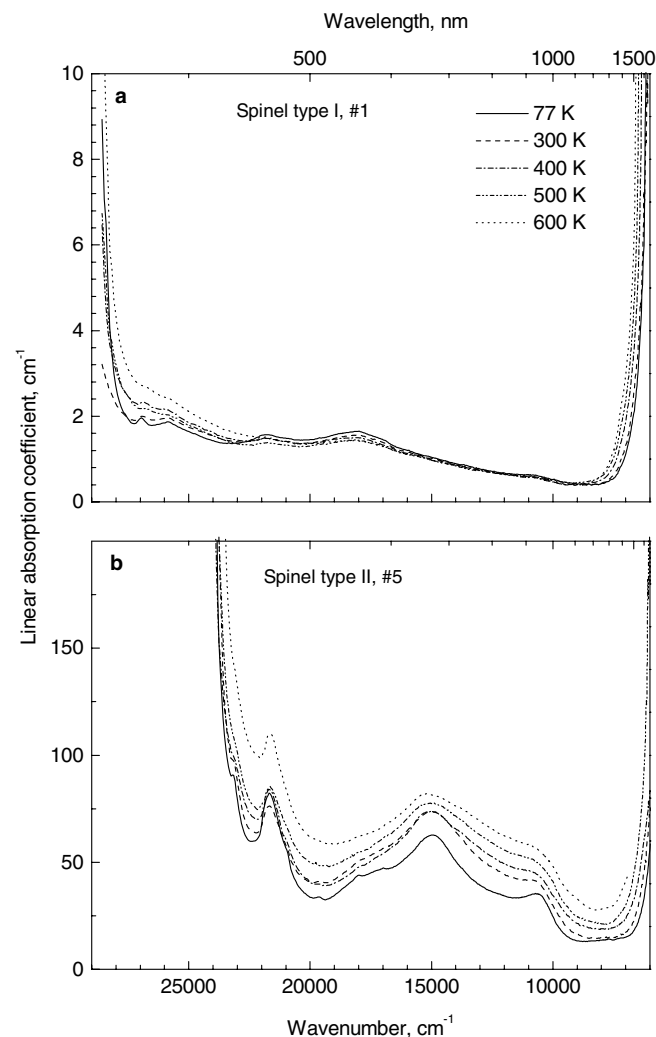


**Fig. 3** Temperature dependent spectra of type I spinel #1 and type II spinel #5. The strongly increasing absorption in the NIR starting from about  $8000$   $\text{cm}^{-1}$  is caused by the high-energy wing of the intense NIR-band system caused by spin-allowed  ${}^5E \rightarrow {}^5T_2$  transition of  ${}^{IV}\text{Fe}^{2+}$  (cf. Fig. 6)



whereas the high-energy edge shifts slightly to lower energies. The curve fitting analysis shows that practically all bands of the group II, *e* to *q*, except *f*, shift with pressure to lower energies. Pressure dependencies of energies of all components bands in spectra of Sp#5, except five weakest ones, *e*, *g*, *h*, *i* and *k* (cf. Fig. 2b), are shown in Fig. 5. As seen from the Figure, the bands *n* and *q* display stronger shifts,  $\Delta v/\Delta P = -28 \text{ cm}^{-1} \times \text{GPa}^{-1}$  and  $-45 \text{ cm}^{-1} \times \text{GPa}^{-1}$ , respectively, than the other bands, *p*, *m*, *g* and, especially, *f*. The latter is practically stable,  $\Delta v/\Delta P = -1.6 \text{ cm}^{-1} \times \text{GPa}^{-1}$ . Inten-

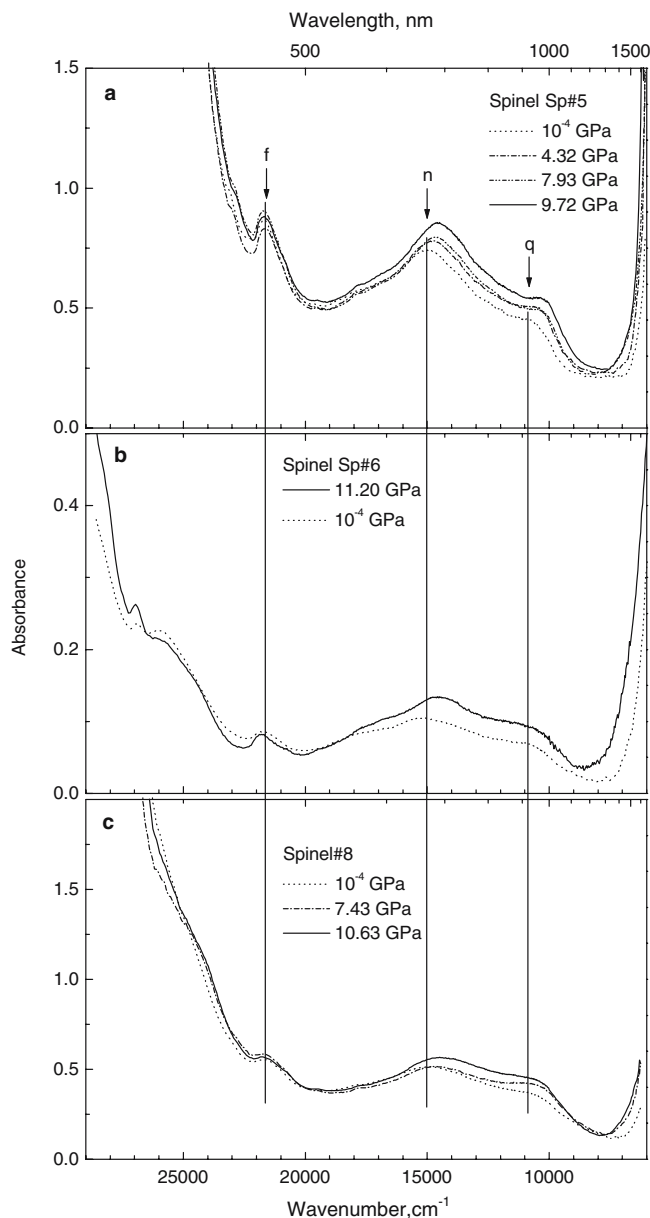


**Fig. 4** Spectra at different pressures of the type II spinels #5, #6 and #8. Three most distinct bands in spectra of type II spinels, *f*, *n* and *q*, are shown by arrows. The vertical lines indicate positions of the bands at ambient pressure. Note that the ordinate values are absorbance,  $\log(I_0/I)$ , due to the fact that thickness of the very thin plates used in the DAC-experiments could not be exactly measured

sities of all bands noticeably increase with pressure; among them *n*, *p* and *q* get the strongest pressure-induced intensifications. Two narrow *b*- and *c*-bands at  $\sim 26000$  and  $27000 \text{ cm}^{-1}$  in spectrum of Sp#5 (Fig. 4b), characteristic for the type I spinels (cf. Figs. 1a and 4b), shift ever slightly to higher energies.

Hydrostatic pressure pronouncedly influences the NIR spin-allowed bands derived from  ${}^5E \rightarrow {}^5T_2$  transition of  ${}^{IV}\text{Fe}^{2+}$ . This effect was studied on two spinels of spinel s.s. - hercynite compositions, Sp#1 and Sp#6, having different iron contents (Table 1). The results obtained on the both samples are rather similar. Therefore, only spectra of Sp#6 in the range  $3500\text{--}7500 \text{ cm}^{-1}$ , measured at different pressures, are shown in Fig. 6. There were four stages of pressure application, which results are seen in Fig. 6, a to d, respectively. First, the spectra were scanned at pressures increasing from the ambient one,  $10^{-4} \text{ GPa}$ , to  $10.22 \text{ GPa}$  (Fig. 6a). At ambient pressure the spin-allowed band of  ${}^{IV}\text{Fe}^{2+}$  is in all respects similar to that described by Taran and Langer (2001) or Rossman and Taran (2001),

First circle: stepwise  $10^{-4} \rightarrow 10.22 \text{ GPa}$  (a),  $10.22 \rightarrow 10^{-4}$  (b). Second circle: stepwise  $10^{-4} \rightarrow 10.70 \text{ GPa}$  (c),  $10.70 \rightarrow 10^{-4}$  (d). Ordinate values as in Fig. 4

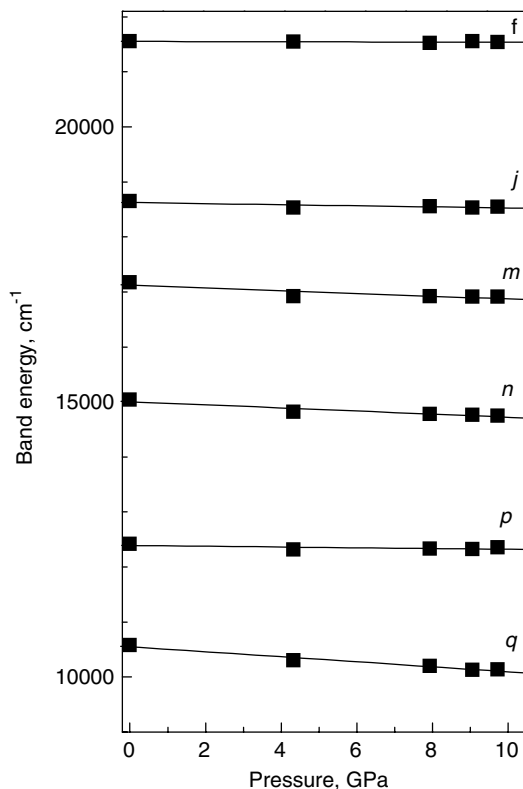
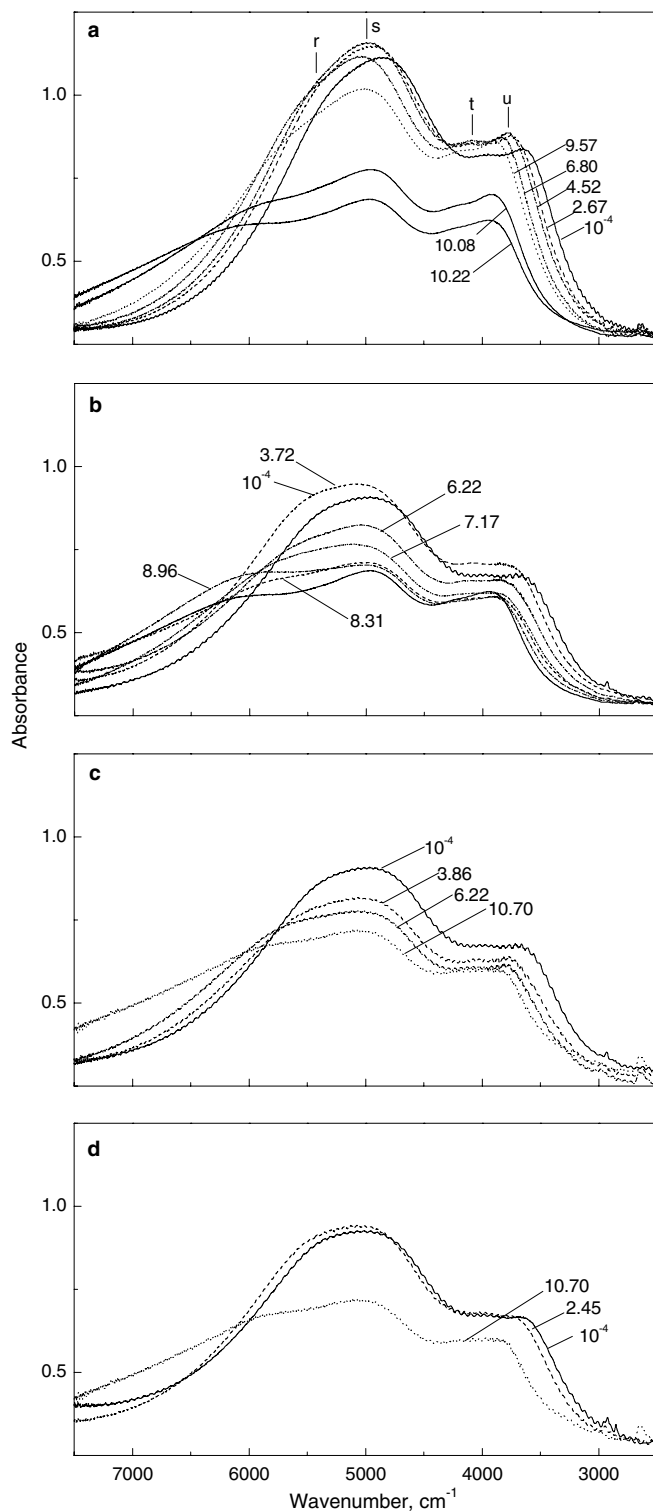


**Fig. 5** Shift with pressure of the energies of the six most intense bands in the spectral range  $28000\text{--}6000 \text{ cm}^{-1}$  of spinel #5, as revealed by curve fitting



showing four distinct features designated as *r*, *s*, *t* and *u*. Energies of these five bands as functions of pressure at this first stage of compression are shown in Fig. 7. As seen from Figs. 6 and 7, at pressures increasing to ca. 4.5 GPa the band shifts monotonously to higher energies, their intensity increases only slightly, the splitting remaining nearly unchanged. At higher pressures, ca. 4.5

to 9.6 GPa, the intensity begins to decrease, the splitting between the *r*- and *s*-components noticeably increases, whereas those between *t*, *u* and *d* slightly decrease. This tendency dramatically enhances in the pressure range from ca. 9.6 to 10.22 GPa: all components significantly decreases in intensity, the splitting between *r*- and *s*-bands strongly increases, those between *s*-, *t*- and *u*-components noticeably decrease.

On the whole the pressure dependence of the band in question, established at the first stage of compression (see above), holds at the second stage, when pressure decreases from 10.22 GPa to ambient one (Fig. 6b). However, we do not observe the entirely reverse behavior especially concerning the intensity of the bands (cf. Figs. 6, a and b). We assume this may be caused by irreversible thinning of the sample (plastic deformation) due to a somewhat non-hydrostatic condition at higher pressures achieved.

At the third stage, a new increasing of pressure from ca.  $10^{-4}$  GPa to 10.7 GPa (Fig. 6c), the dependencies, observed at the first and second stages, hold again, although no strong jump in intensity at pressures between 6.2 and 10.7 GPa, which is distinctly seen in Fig. 6a, is seen. These general tendencies are again well maintained at the fourth stage, at pressure releasing from 10.7 GPa to the ambient one,  $\sim 10^{-4}$  GPa (Fig. 6d).

## Discussion

The high-energy edge, which appears in spectra of all samples studied, type I and II (e.g. Figs. 1), is,

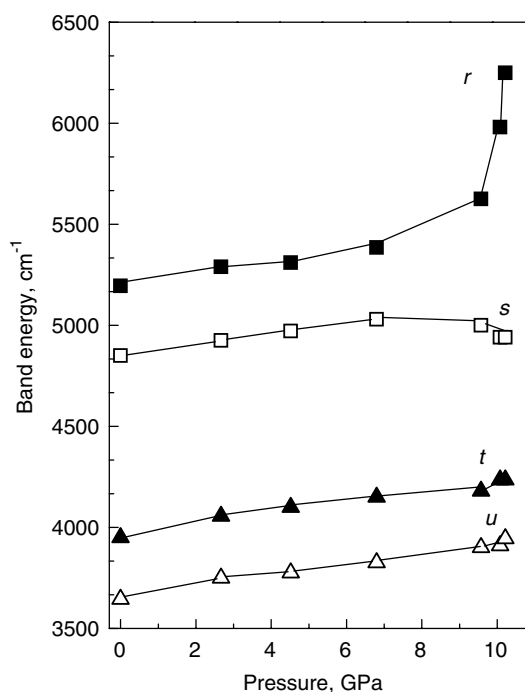


Fig. 7 Pressure dependence of the energies of the split components of the spin-allowed  ${}^3E \rightarrow {}^5T_2$  dd-band of  ${}^{14}\text{Fe}^{2+}$  in the NIR, as derived from the curve analyses of spectra (a) in Fig. 6

judging from chemical compositions of the samples (Table 1), the wing of UV absorption bands caused by oxygen-to-metal electronic charge transfer transitions  $O^{2-} \rightarrow Fe^{3+}$  and  $O^{2-} \rightarrow Fe^{2+}$ . In general, it is stronger in spectra of spinels with higher iron contents.

### Spinel of the group I

As noted in the Result section, iron is the main transition metal component causing spectra and color of the spinels studied. However, the pronounced differences in spectra of type I and II spinels (cf. Fig. 1, a and b) are not caused by different total iron contents alone: another important factors are  $Fe^{3+}/Fe^{2+}$  ratio and distribution of ferrous and ferric ions over the structural sites. Taking into account relatively low total iron contents of Sp#1 and #2, type I (Table 1), one can reasonably assume that these two samples can be regarded as iron-diluted systems in comparison with most of the type II spinels studied. If so, in Sp#1 and #2 interactions between iron ions are less probable than in spinels type II, and the bands, observed in spectra of Sp#1 and #2 (Figs. 1a, 2a), except, perhaps, *q*-band in near IR at  $\sim 10500\text{ cm}^{-1}$ , are to be attributed to electronic spin-forbidden transitions of “isolated”  $^{IV}Fe^{2+}$ . Such an assignment is consistent with many other observations (e.g. Slack et al. 1966; Gaffney 1973; Bukanov et al. 1977; Litsarev et al. 1980). High intensities of these bands in Sp#2 comparing to Sp#1 (Fig. 1a) agrees with higher iron content in the former than in the latter (Table 1).

It should be noted that on the whole the component Gaussian bands in Sp#1, type I, are much broader than in Sp#5, type II (cf. Fig. 2, a and b, Table 2). In particular, three bands, *f*, *i* and *q*, which are assumed to be common in spectra of spinels of both groups, I and II, are significantly broader in Sp#1 than in Sp#5. This suggests that because of a relatively low intensity of the spectrum of Sp#1, smooth character of its spectral curve and rather an uncertain shape of the high-energy edge some component bands in Sp#1 are not revealed by the fitting procedure.

Weak temperature dependencies of the bands in Sp#1 (Fig. 3a) are consistent with their assignment to electronic spin-forbidden *dd* transitions: it is a common observation that when  $Fe^{2+}$  and  $Fe^{3+}$  ions are not involved in exchange-pairing processes, intensity of such bands do not strongly depends on T (e. g. Boksha and Grum-Grzhimailo 1972; Sviridov et al. 1976). Also, spin-forbidden bands of  $Fe^{2+}$  and  $Fe^{3+}$  in spectra of minerals become better resolved at low temperatures.

The energy of band *q*,  $\sim 10550\text{ cm}^{-1}$  (Figs. 2, 3), is too low to be assigned to a spin-forbidden transition of tetrahedral  $Fe^{2+}$  in the spinel structure (Gaffney, 1973). This is very likely a band of the spin-allowed transition  ${}^6A_{1g} \rightarrow {}^4T_{2g}$  of  $^{VI}Fe^{3+}$ . Note, that this band is much stronger and better resolved in spectrum of Sp#5 than in Sp#1. In this juncture the appearance of a weak *n*-band

at around  $15800\text{ cm}^{-1}$  in the spectrum of Sp#2 (Fig. 1a) should be noted. Together with a much stronger high-energy edge than in Sp#1, which, at least partly, should be caused by  $O^{2-} \rightarrow Fe^{3+}$  UV charge transfer band(s), it evidences (see below) of an appreciable  $Fe^{3+}$  content in Sp#2 comparing to Sp#1.

### Spinel of the group II

According to our conception and as follows from the compositions of the spinels studied (Table 1), the bands in the visible and NIR range of the spectra of spinels type II (Fig. 1b, 2b) are caused by electronic transitions of “isolated”  $Fe^{2+}$  and  $Fe^{3+}$ , as well as by pairs of iron ions. Thus, a relatively narrow sharp band *f* with maximum at  $\sim 21700\text{ cm}^{-1}$  (Figs. 1b, Table 2) is typical for  ${}^6A_{1g} \rightarrow {}^4A_{1g}, {}^4E_g$  ( ${}^4G$ ) transition of  $^{VI}Fe^{3+}$  although its energy is significantly lower than in other minerals (cf. Table 5.15 in Burns 1993). However, this band significantly decreases at annealing in reducing conditions (Taran et al. 1987) that strongly supports its assignment to ferric ion. Also, it is close by shape and energy to the band at  $21300\text{ cm}^{-1}$  in synthetic spinel-magnesioferrite solid solution crystals, which Andreozzi et al. (2001) attributed to  ${}^6A_{1g} \rightarrow {}^4A_{1g}, {}^4E_g$  band of  $^{IV}Fe^{3+} - ^{VI}Fe^{3+}$  clusters. A weak pressure dependence of energy of *f*-band (see Results) is also consistent with its assignment to  ${}^6A_{1g} \rightarrow {}^4A_{1g}, {}^4E_g$  ( ${}^4G$ ) transition of  $Fe^{3+}$ , which energy is nearly independent on the crystal field strength (e.g. Dunn et al. 1965; Sviridov et al. 1976). Intensity of the band also does not strongly change with temperature or pressure. By these characteristics it is similar to  ${}^6A_{1g} \rightarrow {}^4A_{1g}$  band of “isolated”  $^{VI}Fe^{3+}$  ions in andradite and epidote (Taran and Langer 2000) or  ${}^6A_{1g} \rightarrow {}^4A_{1g}, {}^4E_g$  band of exchanged-coupled pairs of  $Fe^{3+} - Fe^{3+}$  in tourmaline (Taran and Rossman, 2002). Therefore, at the moment we can not discriminate between “isolated” ions or exchange-coupled pairs of  $Fe^{3+}$  as the cause of band *f* in spectra of spinels of type II. It is not excluded that, at least partly, it may be intensified by exchange-coupled interaction in  $Fe^{3+} - Fe^{3+}$  pairs. On the whole, intensity of the band in question, *f*, does not strictly correlate with the amount of  $Fe^{3+}$  in the spinels studied (cf. Table 1). Especially this is noticeable when spinels of group I and II are compared: at nearly the same  $Fe^{3+}$ -contents intensity of the band in spectra of spinels of the group II is much higher, than in group I. This discrepancy may be due to the fact that in iron-enriched spinels of group II a part of ferric iron enters tetrahedral sites of the spinels structure. In such case, oscillator strength of the electronic transition of tetrahedral ions may be several orders of magnitude higher than in octahedral (e.g. Burns 1993) and the proper absorption bands may be significantly enhanced. Energy of  ${}^6A_1 \rightarrow {}^4A_1, {}^4E$  transition, which is almost independent on Dq (Dunn et al. 1965, Burns 1993), may be very close in  $^{VI}Fe^{3+}$  and  $^{IV}Fe^{3+}$  and, therefore, both transitions may be seen as a single band in the spectra.



Note that in spectra of low-iron spinels of type I, #1 and 2, *f*-band may also be caused by spin-forbidden transitions of tetrahedral  $\text{Fe}^{2+}$ . Therefore, in most cases this relatively sharp distinct peak in spinel spectra is a superposition of two or even three bands of close energies, caused by spin-forbidden transitions of  $^{\text{IV}}\text{Fe}^{2+}$  ( $^3E \rightarrow ^3E(^3G)$ , e.g. Dickson and Smith 1976),  $^{\text{VI}}\text{Fe}^{3+}$  and  $^{\text{IV}}\text{Fe}^{3+}$  ( $^6A_{1g} \rightarrow ^4A_{1g}$ ,  $^4E_g$ , this work).

The *e*-band (Fig. 2b) is, likely,  $^6A_{1g} \rightarrow ^4T_{2g}(^4D)$  transition of  $^{\text{VI}}\text{Fe}^{3+}$  ion, because its intensity roughly correlates with intensity of the *f*-band, assigned above to  $^{\text{VI}}\text{Fe}^{3+}$ . A relatively weak band *c* at  $\sim 20900 \text{ cm}^{-1}$  is, most probably, a split component of the  $^6A_{1g} \rightarrow ^4A_{1g}$ ,  $^4E_g(^4G)$  transition of  $^{\text{VI}}\text{Fe}^{3+}$ .

Origin of the band system *h* to *m* is not quite clear. Note that these bands are more distinct in spectra of low iron samples Sp#6 (Fig. 2b) and #7. Also they are better resolved in low temperature than in room temperature spectra (Fig. 3b). It is very likely that some of them may be caused by spin-forbidden transitions of  $^{\text{IV}}\text{Fe}^{2+}$  (cf. Figs. 2, a and b). Also, we assume that some of these bands may be due to the presence of a trace amount of tetrahedral  $\text{Co}^{2+}$ : in our samples minor amounts of cobalt is detected in the samples #1 to 7 (Table 1, the bottom). Because  $\text{Co}^{2+}$  occupies the tetrahedral position of the structure (e.g. Burns 1993) which lacks a centre of symmetry, spin-allowed bands of  $^{\text{IV}}\text{Co}^{2+}$  may be strong enough to appear in the spectra as weak bands *h* to *m*. As we noticed these bands are more apparent in low- than in high-iron spinels. Therefore, it seems very likely that their intensities do not correlate with iron content. Note also that the intense split band in spectra of both natural and synthetic Co-bearing spinels (Shigley and Stockton, 1984; Rossman 2004) appear at energies close to *j*-, *k*- and *m*-bands in spectra of Fe-bearing spinels.

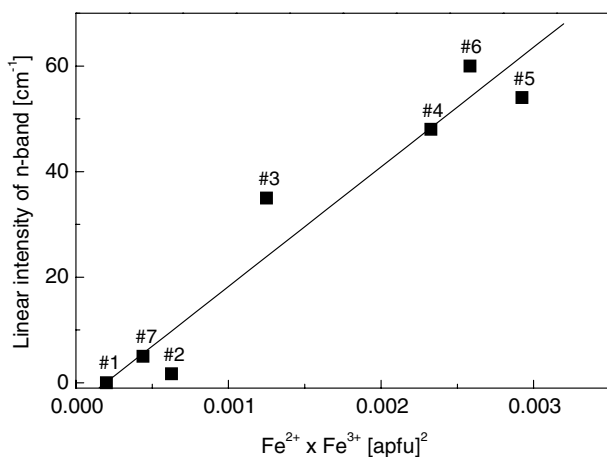


**Fig. 8** Linear intensity of *n*-band, derived by the curve fitting, versus concentration product  $\text{Fe}^{3+} \times \text{Fe}^{2+}$ ,  $\text{apfu}^2$ , in spinel Sp#1 to 7. Spinel #8, which composition is averaged by wet chemical analysis over many grains and does not strictly correspond to the actual samples studied, is not included

Hålenius et al. (2002) observed two broad bands at  $\sim 14500 \text{ cm}^{-1}$  and  $\sim 9500 \text{ cm}^{-1}$  in spectra of synthetic spinels of spinel s.s.–hercynite composition and assigned them to  $^{\text{VI}}\text{Fe}^{2+} + ^{\text{VI}}\text{Fe}^{3+}$  IVCT and  $^{\text{VI}}\text{Fe}^{2+} + ^{\text{VI}}\text{Fe}^{3+}$  ECP. Taking into consideration that the spinels studied contain both  $\text{Fe}^{2+}$  and  $\text{Fe}^{3+}$  ions (Table 1), one could assume that the two relatively intense bands *n* and *q*, at around  $15000 \text{ cm}^{-1}$  and  $10500 \text{ cm}^{-1}$ , respectively, prominent in spectra of spinels type II (Figs. 2b), are related to these bands. However, both *n*- and *q*-, as well as *p*-band, are far much narrower (Table 2) than the above mentioned bands in spectra of the synthetic spinels of  $\text{FWHM} \cong 6000 \text{ cm}^{-1}$  and  $4500 \text{ cm}^{-1}$ , respectively. On the whole, their FWHM-values are atypically low for  $\text{Fe}^{2+} + \text{Fe}^{3+}$  IVCT in minerals (e.g. Burns 1993). In addition, the decrease in intensity of all three bands *n*, *p* and *q* at cooling from room temperature to 77 K (see Results) is not consistent with their assignment to  $^{\text{VI}}\text{Fe}^{2+} + ^{\text{VI}}\text{Fe}^{3+}$  IVCT or  $^{\text{VI}}\text{Fe}^{2+} + ^{\text{VI}}\text{Fe}^{3+}$  ECP. On the contrary, their temperature dependence is just opposite to that observed for  $\text{Fe}^{2+} + \text{Fe}^{3+} \rightarrow \text{Fe}^{3+} + \text{Fe}^{2+}$  IVCT bands in a number of oxygen-based minerals (Smith and Strens 1976, Smith 1977, Taran and Langer 1998). Note that Schmetzer et al. (1989) and Hålenius et al. (2002) assign the IVCT bands in natural and synthetic spinels to electronic transition between ferrous and ferric ions in adjacent equivalent octahedral sites of the spinels structure. Such charge-transfer process is highly symmetric. By the model proposed by Taran and Langer (1998), bands caused by symmetric IVCT transitions should strongly increase by intensity at lowering tem-

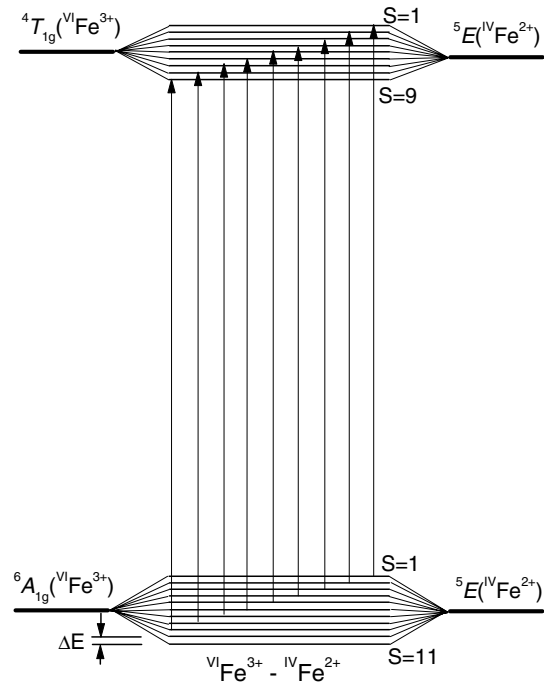


**Fig. 9** Electronic levels of exchange-coupled pair  $^{\text{VI}}\text{Fe}^{3+} - ^{\text{IV}}\text{Fe}^{2+}$ . Spin-allowed transitions are shown by arrows

perature, i.e. they should display temperature dependence emphatically opposite to that of the bands  $n$ ,  $p$  and  $q$  in spinel spectra. Also, as shown by Smith (1978) and Taran et al. (1996), the bands caused by spin-allowed transition of  $\text{Fe}^{2+}$  in  $\text{Fe}^{2+} \text{Fe}^{3+}$  ECP, strongly increase at cooling, thus showing the behavior which is again opposite to those of  $n$ ,  $p$ - and  $q$ -bands in natural spinels type II.

Note that intensities of  $dd$ -bands may increase with temperature when  $3d^N$ -ion occupies centrosymmetric sites in crystalline structures (e.g. Taran et al., 1996; Taran and Langer, 2001). In spinel, where the octahedral site does have a centre of symmetry (point symmetry  $\bar{3}m$ ), such temperature behavior was indeed observed for spin-allowed bands of  $\text{VI}Cr^{3+}$  (Taran et al. 1994). However, the increase in intensity of the  $n$ ,  $p$ - and  $q$ -bands in iron-bearing Sp#4 takes place only in the temperature range 77–300 C while at higher temperatures the integral intensities of the bands in question almost do not change. Such behavior definitely differs from that of spin-allowed bands of  $3d^N$ -ions in centrosymmetric sites (e.g. Taran et al. 1994; Taran and Langer 2001, Taran et al. 2002). Because of this we assume that the bands  $n$ ,  $p$  and  $q$  in the spinel spectra should be caused by another mechanism, whereas the above mentioned dissimilarity with synthetic spinels of s.s.-hercynite composition studied by Hålenius et al. (2002) are due to different  $\text{Fe}^{3+}$ ,  $\text{Fe}^{2+}$ -ordering in natural and synthetic samples. Taran et al. (1987) proposed that  $n$ -band in spectra of natural spinels is caused by  ${}^6A_{1g} \rightarrow {}^4T_{2g}$  transition of  $\text{VI}Fe^{3+}$  intensified by antiferromagnetic exchange interaction in  $\text{VI}Fe^{3+}-\text{IV}Fe^{2+}$  pairs<sup>1</sup>. In Fig. 8 linear intensity of this band versus  $\text{Fe}^{3+}$ - and  $\text{Fe}^{2+}$ -concentration product in spectra of spinels #1 to 7 (Table 1) is shown. An evident tendency to increase with  $\text{Fe}^{3+} \times \text{Fe}^{2+}$  content, fairly well interpolated by linear dependence with  $R=0.965$ , is consistent with  $n$ -band interpretation as caused by  $\text{Fe}^{3+}$ ,  $\text{Fe}^{2+}$  interaction.

Assignment to  $\text{VI}Fe^{3+}-\text{IV}Fe^{2+}$  pair explains also the  $n$ -band weakening at decreasing temperature from 300 to 77 K: in this case electronic transition from the lowest spin sublevel with spin  $S=11$  and from the nearest excited sublevel,  $S=10$ , of the ground state of a pair are forbidden, while those from the other sublevels ( $9 \leq S \leq 1$ ) are allowed (Fig. 9). These series of spin-allowed transitions cause a broad absorption band in the range of  ${}^6A_{1g} \rightarrow {}^4T_{2g}$  transition of  $\text{VI}Fe^{3+}$  in spinel spectra, i. e. the  $n$ -band. At decreasing temperature the electronic population of the lowest sublevel increases at the expense of the higher sublevels. Correspondingly, this causes a decrease of probability of spin-allowed electronic transitions from higher sublevels ( $9 \leq S \leq 1$ )

and, thus, a weakening of the band. According to this model, electron density,  $\rho(E)$ , of an excited sublevel can be described by the expression

$$\rho(E) \sim \exp(n \cdot \Delta E/k),$$

where  $n = 1, 2, \dots, 11$  is the serial number of a sublevel,  $\Delta E$  is the energy gap between the sublevels (Fig. 9),  $k$  is the Boltzmann constant and  $T$  is absolute temperature. The fact that intensity of band  $n$  increases mostly in the range from ca. 77 to ca. 300°C, but almost does not change at higher temperatures evidences of a relatively small energy interval,  $\Delta E$ , between the split sublevels (Fig. 9) when compared with the thermal excitation energy  $kT$  at  $T \approx 300$  K. Room temperature,  $\sim 300$  K, is high enough to pump up most of the electron density from the ground and nearest-to-ground level to higher ones of  $S \geq 2$ . Therefore, at  $T > 300$  K only further redistribution of the electron density between the higher sublevels,  $11 \geq S \geq 2$ , takes place, which, however, does not much influence intensity of the band.

Note that the relation of the  $n$ -band to  $\text{Fe}^{3+}$  content is well supported by the results of annealing of spinels at reducing conditions which results to a significant weakening of the band due to reducing  $\text{VI}Fe^{3+}$  to  $\text{VI}Fe^{2+}$  (Dickson and Smith 1976, Taran et al. 1987). Also, a slight shift of  $n$ -band to higher energies at increasing temperature (see Results) is consistent with its assignment to  ${}^6A_{1g} \rightarrow {}^4T_{2g}$  transition of  $\text{VI}Fe^{3+}$ , which energy, according to the Tanabe-Sugano diagram for electronic  $d^5$ -configuration (e.g. Dunn et al. 1965, Sviridov et al. 1976, Burns 1993), should increase with decreasing  $Dq$  caused by thermally induced expanse of the coordination octahedron of  $\text{Fe}^{3+}$ .

A noticeable weakening of the band  $q$  at cooling (Fig. 3b, Table 2) suggests that like  $n$ -band it may be caused by an electronic transition in  $\text{VI}Fe^{3+}-\text{IV}Fe^{2+}$  pair. Taking into account the energy of the band,  $\sim 10550 \text{ cm}^{-1}$ , it may be attributed to the  ${}^6A_{1g} \rightarrow {}^4T_{1g}$  transition of  $\text{VI}Fe^{3+}$  (cf. Table 5.15 of Burns 1993), intensified by the exchange interaction. A scheme of the energy levels of the pair in this case would be similar to that in Fig. 9 for the  ${}^6A_{1g} \rightarrow {}^4T_{2g}$  transition.

At annealing in reducing conditions  $q$ -band seems to increase (Dickson and Smith 1976, Taran et al. 1987). We believe that in this case a new band of the spin-allowed transition of  $\text{VI}Fe^{2+}$ , close by energy to  $q$ -band, appears and rises due to increasing concentration of  $\text{VI}Fe^{2+}$  at the expense of  $\text{VI}Fe^{3+}$ . Therefore, it is very likely that in this spectral range two bands occur:  $q$ -band, which is caused by  ${}^6A_{1g} \rightarrow {}^4T_{1g}$  transition of  $\text{VI}Fe^{3+}$  enhanced by the exchange interaction, and spin-allowed band  ${}^5T_{2g} \rightarrow {}^5E_g$  of  $\text{VI}Fe^{2+}$ , which appears in thermally reduced spinels.

The band  $p$ , which also decreases at cooling (see Results), may be a split component of the  ${}^6A_{1g} \rightarrow {}^4T_{1g}$  transition of  $\text{VI}Fe^{3+}$ , caused by trigonal distortion of the octahedral site in the spinel structure (the point symmetry  $\bar{3}mm$ ).

<sup>1</sup>It should be noted that energy of exchange-coupling interaction in pairs of  $3d$ -ions is small when compare with difference of energies of the ground and first excited states of "isolated" ions. This evidences that the ions in pairs keep to a great extent their individual electronic features (e.g. Cherepanov and Men', 1970).

Interpretation of  $n$ -,  $p$ - and  $q$ -bands as electronic  ${}^6A_{1g} \rightarrow {}^4T_{1g}$  and  ${}^6A_{1g} \rightarrow {}^4T_{2g}$  transitions of  $\text{Fe}^{3+}$  intensified by the exchange interaction, is strongly supported by investigation of spinel spectra in DAC-experiments at different pressures (Figs. 4, 5). First, by pressure-induced shifts to lower energies these bands significantly differ from IVCT or spin-allowed bands in minerals. Indeed, as found by Taran and Langer (1998), under pressure the IVCT bands either do not shift at all or shift ever slightly to higher energies, *i.e.* display the pressure behavior quite different from those observed for the  $n$ ,  $p$  and  $q$  bands in spinels. The spin-allowed  $dd$ -bands, both of “isolated”  $\text{Fe}^{2+}$  or coupled with adjacent  $\text{Fe}^{3+}$ , significantly shift to higher energies at pressure (*e.g.* Langer 1990, Taran et al. 1996, Taran and Rossman 2002), *i.e.* again show the pressure-induced behaviors opposite to those observed for bands  $n$ ,  $p$  and  $q$  in spinel spectra. Second, the “red” shifts of these bands at pressure (Fig. 4, 5) are well consistent with their assignment to the spin-forbidden transitions  ${}^6A_{1g} \rightarrow {}^4T_{2g}$  and  ${}^6A_{1g} \rightarrow {}^4T_{1g}$  of  $\text{Fe}^{3+}$ . Indeed, by theory, in difference to spin-allowed bands of  $3d^N$ -ions, the energies of the spin-forbidden bands  ${}^6A_{1g} \rightarrow {}^4T_{2g}$  and  ${}^6A_{1g} \rightarrow {}^4T_{1g}$  of  $\text{Fe}^{3+}$  relatively slowly decrease when the crystal field strength  $Dq$  of  $\text{Fe}^{3+}$  increases (*e.g.* Dunn et al. 1965).  $Dq$  strongly depends on mean metal-oxygen distances  $R$  in  $3d^N$ -ion centered coordination polyhedra as  $1/R^5$ . Since hydrostatic pressure shortens interatomic distances in crystal structure, the pressure-induced shifts of  ${}^6A_{1g} \rightarrow {}^4T_{2g}$  and  ${}^6A_{1g} \rightarrow {}^4T_{1g}$  bands of  $\text{Fe}^{3+}$  to lower energies is expectable. Note that just such pressure induced behavior was observed by Taran and Langer (2000) for  ${}^6A_{1g} \rightarrow {}^4T_{2g}$  band of  $\text{Fe}^{3+}$  in epidote.

A noticeable intensification of  $n$  to  $q$  bands in the spinel spectra with increasing pressure (Fig. 4) may be explained by increase of the exchange interaction in  ${}^{\text{VI}}\text{Fe}^{3+}-{}^{\text{IV}}\text{Fe}^{2+}$  ECP due to shortening of  ${}^{\text{VI}}\text{Fe}^{3+}-{}^{\text{IV}}\text{Fe}^{2+}$  distances at pressure and, therefore, higher overlapping of the Fe-Fe bonds.

Although we assume that the  $f$ -band in spectra of the spinel studied is caused by spin-forbidden transition of  ${}^{\text{VI}}\text{Fe}^{3+}$  (see above), a weak temperature dependence of its intensity suggests that unlikely to bands  $n$ ,  $p$  and  $q$ , which are also caused by spin-forbidden transitions  ${}^6A_{1g} \rightarrow {}^4T_{2g}$  and  ${}^6A_{1g} \rightarrow {}^4T_{1g}$  of  ${}^{\text{VI}}\text{Fe}^{3+}$ , the  $f$ -band is not enhanced by exchange-coupled interaction with neighboring  ${}^{\text{IV}}\text{Fe}^{2+}$ . This may be the reason why relative intensity of band  $f$  vs.  $n$ -,  $p$ - and  $q$ -bands strongly varies in the samples studied (cf. spectra in Fig. 4): this may be caused by different concentrations of  ${}^{\text{VI}}\text{Fe}^{3+}-{}^{\text{IV}}\text{Fe}^{2+}$  ECP and “isolated”  $\text{Fe}^{3+}$  in the samples. At the moment we can not explain a reason for such “discrimination” of  ${}^6A_{1g} \rightarrow {}^4A_{1g}$ ,  ${}^4E_g$ -transition vs.  ${}^6A_{1g} \rightarrow {}^4T_{2g}$  and  ${}^6A_{1g} \rightarrow {}^4T_{1g}$ . From the published data on spectroscopy of  $\text{Fe}^{3+}-\text{Fe}^{3+}$  ECP, for instance (*e.g.* Krebs and Maisch 1971, Ferguson and Fielding 1972, Rossman 1975, 1976), which are quite common in  $\text{Fe}^{3+}$ -concentrated crystals, we only learn that far not all electronic transitions of  $\text{Fe}^{3+}-\text{Fe}^{3+}$  pairs equally gain intensity from the

exchange interaction. Perhaps, a similar situation takes place in  ${}^{\text{VI}}\text{Fe}^{3+}-{}^{\text{IV}}\text{Fe}^{2+}$  pair in spinels: the bands originating from electronic transitions  ${}^6A_{1g} \rightarrow {}^4T_{1g}$  and  ${}^6A_{1g} \rightarrow {}^4T_{2g}$  of  $\text{Fe}^{3+}$  gain much more intensity from the exchange interaction than the band originating from  ${}^6A_{1g} \rightarrow {}^4A_{1g}$ ,  ${}^4E_g$  transition. It should also be noted that, as far as we are aware, such type of exchange-coupled pair,  ${}^{\text{VI}}\text{Fe}^{3+}-{}^{\text{IV}}\text{Fe}^{2+}$ , where spin-forbidden transitions of  $\text{Fe}^{3+}$  are intensified by exchange interaction, was not yet found in minerals.

#### Pressure dependence of the spin-allowed band of ${}^{\text{IV}}\text{Fe}^{2+}$

The pressure dependence of the intense broad structured bands in the near IR of spectra of natural or synthetic  $\text{Fe}^{2+}$ -bearing spinels, attributed to the spin-allowed transition  ${}^5E \rightarrow {}^5T_2$  of  ${}^{\text{IV}}\text{Fe}^{2+}$ , is, as far as we know, not yet studied. Since the tetrahedral site in the spinel structure is not distorted, point symmetry  $\bar{4}3m3m$  (*e.g.* Yamanaka and Takéuchi 1983), one should expect appearance of a single band, but this not the case – at least four components,  $r$  to  $u$ , appear in the range of  ${}^5E \rightarrow {}^5T_2$  transition of  ${}^{\text{IV}}\text{Fe}^{2+}$  (Fig. 6). The observed splitting of the  ${}^5E \rightarrow {}^5T_2$  band is attributed to a dynamic Jahn-Teller effect (Slack et al. 1966; Rossman and Taran 2001; Taran and Langer 2001; Skogby and Hålenius 2003). This effect is assumed to be a cause of rather unusual temperature behavior of the spin-allowed band of  ${}^{\text{IV}}\text{Fe}^{2+}$  in spinel when compared to those of  $\text{Fe}^{2+}$  in octahedral sites (Taran and Langer 2001).

Pressure usually causes a shift of the spin-allowed bands  ${}^5T_{2g} \rightarrow {}^5E_g$  of octahedral  $\text{Fe}^{2+}$  to higher energies and decrease of their splitting, thus reflecting two simultaneous pressure-induced processes: shortening of the Fe-O distances and decrease of distortion of  $\text{FeO}_6$  octahedra (*e.g.* Hazen and Finger 1982). In case of Jahn-Teller-distorted complexes, as recently shown by Aguado et al. (2002, 2003) on  $\text{NaMnF}_4$  crystals, pressure behavior of spin-allowed  $dd$  bands is somewhat different. The spin-allowed bands of  ${}^{\text{VI}}\text{Mn}^{3+}$ , derived from  ${}^5E_g \rightarrow {}^5T_{2g}$  transition, also shift to higher energy reflecting the fact of shortening of Mn-O distances in  $\text{MnO}_6$ -octahedra at pressure. However, the splitting of the bands does not decrease. On the contrary, it slightly increases, although X-ray diffraction structural refinement indicates a significant decrease of tetragonal distortion of  $\text{MnO}_6$ -octahedra. Aguado et al. (2002, 2003) explain this by pressure-induced enhancement of Jahn-Teller electron-lattice coupling.

As seen from Fig. 7 (see also the Results section), at moderate pressures (up to  $\sim 7$  GPa) a similar situation is observed for  ${}^5E \rightarrow {}^5T_2$  band of  ${}^{\text{IV}}\text{Fe}^{2+}$  in spinel, although in this case Jahn-Teller effect has a dynamic character in difference to  $\text{NaMnF}_4$ , where the Jahn-Teller distortion is static. At least, the pressure induced behavior of the spin-allowed band of  $\text{Fe}^{2+}$  in tetrahedral sites of the spinel structure emphatically differs from that of  ${}^{\text{VI}}\text{Fe}^{2+}$  in octahedral sites of minerals. In the

latter case a significant pressure-induced decrease of splitting of the  ${}^5E_g$ -state of  $\text{Fe}^{2+}$ , caused by distortion of octahedral coordination, usually takes place (e.g. Abu-Eid 1976; Smith and Langer 1982, Taran and Rossman 2002; Taran and Langer 2003). However, in spinel this is not the case (see Results). This evidences that either dynamic distortion of  $\text{FeO}_4$ -tetrahedra does not significantly change at pressure or, like  $\text{NaMnF}_4$ , enhancement of electron-lattice coupling coefficients takes place (Aguardo et al. 2003). By analogy with  $\text{NaMnF}_4$  compound we are inclined to believe that in spinel the latter effect, i.e. an enhancement of electron-lattice coupling is prevalent. It is less probable that with increasing pressure an intensification of dynamic distortion of  $\text{FeO}_4$ -tetrahedron takes place.

At higher pressures, more than ca. 9.5 GPa, the situation in spinel becomes more complicated (see Results), but whether this is a manifestation of pressure effect on the Jahn-Teller center  ${}^{\text{IV}}\text{Fe}^{2+}$ , or is caused by non-hydrostatic, uniaxial, compressing of the sample, or both, we can not decide. Particularly, we estimate that at the highest pressure of the first stage of compression, the pressure determined on different ruby chips in the gasket chamber differs by 5%, i.e.  $10 \pm 0.5$  GPa, thus indicating non-hydrostatic conditions. But at the following stages of pressure application such a large variation was never observed. For instance, at the third stage the highest pressure inhomogeneity was estimated as only  $\pm 0.1$  GPa. Therefore, it seems that the observed increase of splitting of the  ${}^5T_2$ -state of  ${}^{\text{IV}}\text{Fe}^{2+}$  at high pressures does not strongly depend on inhomogeneity of P (cf. Figs. 10, a-d). It may be explained by the effect of vibronic enhancement of structural distortion caused by non-hydrostatic, uniaxial, compressing of the sample. Indeed, by theory (e.g. Bersuker 1996), the magnitude of such outer-induced distortion of a Jahn-Teller center is controlled mainly by values of electron-lattice coupling coefficients (which, as we assume, increase at pressure (see above)), and does not dependent on the perturbation magnitude. This is consistent with our observation in spinel. In such case even a small perturbation of tetrahedral  $\text{Fe}^{2+}$ -centered site in spinel, induced by non-hydrostatic compression, significantly increases its dynamic distortion what is seen as the increase of the  ${}^5T_2$ -state splitting (Fig. 7). In case of a strong enough vibronic coupling this can even stabilize one of the distorted configurations, i.e. can cause a relatively high static distortion of  ${}^{\text{IV}}\text{Fe}^{2+}$ -bearing sites (Bersuker 1996). X-ray diffraction structural refinements of  ${}^{\text{IV}}\text{Fe}^{2+}$ -bearing spinels at pressures higher than ca. 9.5 GPa would be very helpful to verify this assumption. We consider also that spectroscopic high-pressure experiments with other pressure transmitting mediums are very desirable.

Keeping in mind a rather unusual behavior of the spin-allowed bands of  $\text{Fe}^{2+}$  in spinel with temperature (Taran and Langer 2003) we believe that this and the pressure-induced effects on  $\text{Fe}^{2+}$  in spinels invokes more detailed study, quantification and, especially, theoretical analysis.

One can estimate a compressibility of  $3d^N$ -ion-centered octahedron from optical absorption spectra measured at different pressures. When  $3d^N$ -ion is  ${}^{\text{VI}}\text{Cr}^{3+}$  or  ${}^{\text{VI}}\text{Fe}^{2+}$ , this usually gives results quite comparable with those obtained by X-ray diffraction structural refinements (e.g. Langer et al. 1997, Taran and Langer 2003). In case of  ${}^{\text{VI}}\text{Fe}^{2+}$  one has to ignore a splitting of the ground electronic  ${}^5T_{2g}$ -state, which can not be obtained from the spectra (Taran and Langer 2003). In similar way we evaluated the tetrahedral modulus of  $\text{Fe}^{2+}$  in spinel from the spectra, measured at pressures from  $10^{-4}$  to 6.8 GPa (Fig. 6a), i.e. in the pressure range where we expect more or less hydrostatic conditions (see above). It gives  $k_{\text{tet}}^{\text{spectr}} \approx 273$  GPa, which is much higher than obtained from the synchrotron X-ray powder diffraction data for synthetic  $\text{MgAl}_2\text{O}_4$ ,  $190.8 \pm 1.2$  GPa (Levy et al. 2003). The latter value is, in fact,  $k_{\text{bulk}}$ , but compression of  $\text{MgAl}_2\text{O}_4$  spinel occurs with a negligible change of the fractional coordinate of oxygen. Therefore, the structural behavior of spinel under compression is mainly governed by shrinkage of the cell edge (Levy et al. 2003), i.e. in this case  $k_{\text{bulk}} \approx k_{\text{tet}}^{\text{XRD}} k_{\text{oct}}^{\text{XRD}}$ .

For synthetic gahnite,  $\text{ZnAl}_2\text{O}_4$ ,  $k_{\text{tet}}^{\text{XRD}}$  can be calculated from the mean linear tetrahedral compressibility  $\beta_1$ ,  $k_{\text{tet}}^{\text{XRD}} = 1/3\beta_1$  (e.g. Langer 1990), determined by high-pressure X-ray diffraction structural study as  $0.00188(8)$   $\text{GPa}^{-1}$  (Levy et al. 2001). It gives  $k_{\text{tet}}^{\text{XRD}} \cong 177 \pm 7$  GPa, close to that of  $\text{MgAl}_2\text{O}_4$ ,  $190.8 \pm 1.2$  GPa.

A significant difference between  $k_{\text{tet}}^{\text{spectr}}$ , 273 GPa, obtained from the spectra, and  $k_{\text{tet}}^{\text{XRD}}$ ,  $\sim 180$  GPa and 190 GPa, obtained from X-ray powder diffraction data (Levy et al. 2001, 2003), may be due to the fact that ignoring the splitting of the ground  ${}^5E$ -state of  ${}^{\text{VI}}\text{Fe}^{2+}$  we overestimate  $10Dq$ -value of  ${}^{\text{IV}}\text{Fe}^{2+}$  calculated from the barycenter of the excited  ${}^5T_2$ -level (cf. Taran and Langer 2003). Note that in case of tetrahedral complexes of  $\text{Fe}^{2+}$  this may cause much larger deviations from the true value than in case of octahedral  $\text{Fe}^{2+}$ . The discrepancy between  $k_{\text{tet}}^{\text{spectr}}$  and  $k_{\text{tet}}^{\text{XRD}}$  of  $\text{FeO}_4$ -tetrahedra in spinel may also arise from a dynamic Jahn-Teller effect intrinsic to  ${}^{\text{VI}}\text{Fe}^{2+}$  in the spinel structure.

## Conclusions

By color and electronic absorption spectra natural spinels of the spinel s.s.-hercynite and gahnite-hercynite series may be divided into two types. Light-violet type I spinels belong to low-iron spinel s.s.-hercynite series. Their spectra are mainly caused by spin-forbidden and spin-allowed electronic  $dd$ -transitions of "isolated"  $\text{Fe}^{2+}$  in tetrahedral sites of the spinel structure. Electronic spectra of green and bluish-green high-iron spinels type II of both spinel s.s.-hercynite and gahnite-hercynite series are predominantly caused by electronic  $dd$ -transitions both of  ${}^{\text{IV}}\text{Fe}^{2+}$  and  ${}^{\text{VI}}\text{Fe}^{3+}$ , as well as of exchange-coupled pairs of these ions. Particularly, temperature and pressure behaviors of absorption bands at  $\sim 21600$   $\text{cm}^{-1}$ ,  $15000$   $\text{cm}^{-1}$  and  $\sim 10500$   $\text{cm}^{-1}$ , intense in



electronic absorption spectra of type II spinels, evidence that these bands are, most probably, caused by electronic spin-forbidden transitions  ${}^6A_{1g} \rightarrow {}^4A_{1g}$ ,  ${}^4E_g$ ,  ${}^6A_{1g} \rightarrow {}^4T_{2g}$  and  ${}^6A_{1g} \rightarrow {}^4T_{1g}$ , respectively, of  ${}^{VI}Fe^{3+}$ . In Fe-enriched spinels of type II the former bands may be enhanced also by  ${}^6A_{1g} \rightarrow {}^4A_{1g}$ ,  ${}^4E_g$  transition of  ${}^{IV}Fe^{3+}$ . The bands  ${}^6A_{1g} \rightarrow {}^4T_{2g}$  and  ${}^6A_{1g} \rightarrow {}^4T_{1g}$  of  ${}^{VI}Fe^{3+}$  are found to be strongly intensified by exchange-coupling interaction with neighboring  ${}^{IV}Fe^{2+}$  ions. In contrast to synthetic  $Fe^{3+}$ -bearing spinel of spinel s.s.-hercynite compositions of different  $Fe^{3+}$ ,  $Fe^{2+}$  ordering (Hålenius et al. 2002), the bands, which may be interpreted as  $Fe^{2+} Fe^{3+}$  IVCT or  ${}^{VI}Fe^{2+}$ ,  ${}^{IV}Fe^{3+}$  ECP, are not identified.

Due to a dynamic Jahn-Teller effect, pressure-induced behavior of spin-allowed bands of  ${}^{IV}Fe^{2+}$  in spinels in the NIR range significantly differs from those of octahedral  $Fe^{2+}$  in various minerals. In difference to  ${}^{VI}Fe^{2+}$  in many oxygen-based minerals the splitting of the spin-allowed bands derived from  ${}^5E \rightarrow {}^5T_2$  transition of  ${}^{IV}Fe^{2+}$  in spinels does not decrease with pressure. On the contrary, it markedly increases showing that values of vibronic coupling coefficients of  ${}^{IV}Fe^{2+}$  rise. Also, the values of tetrahedral moduli of  $Fe^{2+}$  in spinel, evaluated from high-pressure spectra and X-ray diffraction structural refinements, are significantly different that again may be caused by a dynamic Jahn-Teller effect of  ${}^{IV}Fe^{2+}$  in the spinel structure.

**Acknowledgements** The German Science Foundation, Bonn-Bad Godesberg, generously supported this work through traveling grants to the senior author. Two referees, A. Della Giusta and an anonymous referee, gave very reasonable remarks and suggestions which allowed significant improving the paper.

## References

- Abu-Eid RM (1976) Absorption spectra of transition metal-bearing minerals at high pressures. In: Strens RGJ (ed) *The Physics and Chemistry of Minerals and Rocks*. J Wiley, New York, pp 641–675
- Aguado F, Rodr ygu ez F, N n ez P (2002) Pressure effects on the cooperative Jahn-Teller distortion in  $AMnF_4$  ( $A = Na, Tl$ ). *High Pressure Research* 22:641–675
- Aguado F, Rodr ygu ez F, N n ez P (2003) Pressure effects on  $NaMnF_4$ : Structural correlations and Jahn-Teller effect from crystal-field spectroscopy. *Phys Rev B* 67:205101
- Andreozzi GB, H lenius U, Skogby H (2001) Spectroscopic active  ${}^{IV}Fe^{3+} - {}^{VI}Fe^{3+}$  clusters in spinel-magnesioferrite solid solution crystals: a potential monitor for ordering in oxide spinels. *Phys Chem Minerals* 28:435–444
- Bersuker IB (1996) *Electronic Structure and Properties of Transition Metal Compounds: Introduction to the Theory*. Wiley-Interscience, NY
- Boksha ON, Grum-Grzhimailo SV (1972) Investigations of optical spectra of crystals with ions of the iron group at room and low temperatures. Moscow, Nauka (in Russian)
- Bukanov UV, Platonov AN, Taran MN (1977) Color of gem quality spinels from the Kuhilal deposit. *Zap Vsesoyuz Min Obshchestva* 61:565–571 (in Russian)
- Burns RG (1993) *Mineralogical Applications of Crystal Field Theory*, 2nd edn. Cambridge University Press, Cambridge
- Cherepanov VI, Men' AN (1970) Spectra of pairs of impurity ions and super-exchange interactions in magnetically dilute crystals. In: *Spectroscopy of Crystals*. Nauka, Moscow, pp 62–73 (in Russian)
- Dickson BL, Smith G (1976) Low temperature optical absorption and M ssbauer spectra of staurolite and spinel. *Canadian Mineral* 14:206–215
- Dunn TM, McClure DS, Pearson RG (1965) *Some Aspects of Crystal Field Theory*. Harper & Row, New York
- Ferguson J, Fielding PE (1972) The origins of the colours of natural yellow, blue, and green sapphires. *Australian J Chem* 25:1371–1385
- Gaffney ES (1973) Spectra of tetrahedral  $Fe^{2+}$  in  $MgAl_2O_4$ . *Phys Rev B* 8:3484–3486
- H lenius U, Skogby H, Andreozzi GB (2002) Influence of cation distribution on the optical absorption spectra of  $Fe^{3+}$ -bearing spinel s.s.-hercynite crystals: evidence for electron transitions in  ${}^{VI}Fe^{2+} - {}^{VI}Fe^{3+}$  clusters. *Phys Chem Minerals* 29:319–330
- Hazen RM, Finger LW (1982) *Comparative Crystal Chemistry: temperature, pressure, composition and the variation of crystal structure*. John Wiley & Sons, New York
- Krebs JJ, Maisch WG (1971) Exchange effects in the optical-absorption spectrum of  $Fe^{3+}$  in  $Al_2O_3$ . *Phys Review B* 757–769
- Langer K (1990) High pressure spectroscopy. In: Monttana A, Burrigato F (eds) *Absorption Spectroscopy in Mineralogy*. Elsevier, pp 228–284
- Langer K, Taran MN, Platonov AN (1997) Compression moduli of  $Cr^{3+}$ -centered octahedra in a variety of oxygen-based rock-forming minerals. *Phys Chem Minerals* 24:109–114
- Levy D, Pavese A, Sanni A., Rischiedda V (2001) Structure and compressibility of synthetic  $ZnAl_2O_4$  (gahnite) under high-pressure conditions, from synchrotron X-ray powder diffraction. *Phys Chem Minerals* 28:612–618
- Levy D, Pavese A, Hanfland M (2003) Synthetic  $MgAl_2O_4$  (spinel) at high-pressure conditions (0.0001–30 GPa): A synchrotron X-ray powder diffraction study. *Amer Mineral* 88:93–98
- Litsarev MA, Platonov AN, Taran MN, Polshin EV (1980) A violet spinel from South-Western Pamir. In: *Gems and Colored Stones*. Moscow, Nauka, pp 211–220 (in Russian)
- Rossmann GR (1975) Spectroscopic and magnetic studies of ferric iron hydroxy sulfates: Intensification of color in ferric iron clusters bridged by a single hydroxide ion. *Amer Mineral* 60:698–704
- Rossmann GR (1976) Spectroscopic and magnetic studies of ferric iron hydroxy sulfates: The series  $Fe(OH)SO_4 \cdot nH_2O$  and jarosite. *Amer Mineral* 61:398–404
- Rossmann GR (2004) Mineral Spectroscopy Server. <http://minerals.gps.caltech.edu>
- Rossmann GR, Taran MN (2001) Spectroscopic standards for four- and five-coordinated  $Fe^{2+}$  in oxygen-based minerals. *American Mineralogist* 86:896–903
- Schmetzer K, Haxel C, Amthauer G (1989) Color of natural spinels, gahnospinel and gahnites. *N Jb Mineral Abh* 160:159–180
- Shigley JE, Stockton CM (1984) Cobalt-blue gem spinels. *Gems & Gemology* 20:34–41
- Siroshtan RI, Polovko NI, Bondareva NM, Kravchenko GL, Parfenova AY, Sokirko L, Spivak SD (1976) Minerals of carbonate rocks of the Ukrainian shield. *Kiev Naukova Dumka* (in Russian)
- Skogby H, H lenius U (2003) An FTIR study of tetrahedrally coordinated ferrous ions in the spinel-hercynite solid solution. *Amer Mineral* 88:489–492
- Slack GA, Ham FS, Chrenko RM (1966) Optical absorption spectra of tetrahedral  $Fe^{2+}$  ( $3d^6$ ) in cubic ZnS, CdTe and  $MgAl_2O_4$ . *Phys Rev* 152:376–402
- Smith G (1977) Low-temperature optical studies of metal-metal charge-transfer transitions in various minerals. *Canadian Mineral* 15:500–507
- Smith G (1978) A reassessment of the role of iron in the 5,000–30,000  $cm^{-1}$  region of the electronic absorption spectra of tourmaline. *Phys Chem Minerals* 3:343–373



- Smith G, Langer K (1982) Single crystal spectra of olivines in the range 40,000–50,000  $\text{cm}^{-1}$  at pressures up to 200 kbars. *Amer Mineral* 67:343–348
- Smith G, Strens RGJ (1976) Intervalence transfer absorption in some silicate, oxide and phosphate minerals. In: Strens RGJ (ed) *The Physics of Minerals and Rocks*. Wiley, New York, pp 583–612
- Sviridov DT, Sviridova RK, Smirnov JF (1976) Optical spectra of transition metal ions in crystals. Moscow, Nauka (in Russian)
- Taran MN, Langer K (1998) Temperature and pressure dependencies of intervalence charge transfer bands in spectra of Fe- and Ti-bearing oxygen-based minerals. *N Jb Min Abh* 172:325–346
- Taran MN, Langer K (2000) Electronic absorption spectra of  $\text{Fe}^{3+}$  in andradite and epidote at different temperatures and pressures. *Eur J Mineralogy* 12:7–15
- Taran MN, Langer K (2001) Electronic absorption spectra of  $\text{Fe}^{2+}$  ions in oxygen-based rock-forming minerals at temperatures between 297 and 600 K. *Phys Chem Minerals* 28:199–210
- Taran MN, Langer K (2003) Single-crystal high-pressure electronic absorption spectroscopic study of natural orthopyroxenes. *Eur J Mineral* 15:689–695
- Taran MN, Rossman GR (2002) High-temperature, high-pressure optical spectroscopic study of ferric-iron-bearing tourmaline. *American Mineralogist* 87:1148–1153
- Taran MN, Platonov AN, Pol'shin EV, Matsyuk SS (1987) Optical spectra and coloration of natural spinels of the (Mg, Zn, Fe)(Al, Fe)<sub>2</sub>O<sub>4</sub> composition. *Min Zhurnal* 9:3–15 (in Russian)
- Taran MN, Kirilov SP, Vishnevski AA (1988) Optical spectra and coloration of spinels from carbonatite rocks of the upper South Bug river. *Min Sbornik* 42(2):7–11 (in Russian)
- Taran MN, Langer K, Platonov AN, Indutny VV (1994) Optical absorption investigation of  $\text{Cr}^{3+}$  ion-bearing minerals in the temperature range 77–797 K. *Phys Chem Minerals* 21:360–372
- Taran MN, Langer K, Platonov AN (1996) Pressure- and temperature-effects on exchange-coupled-pair bands in electronic spectra of some oxygen-based iron-bearing minerals. *Phys Chem Mineral* 23:230–236
- Taran MN, Langer K, Geiger CA (2002) Single-crystal electronic absorption spectroscopy of synthetic chromium-, cobalt-, and vanadium-bearing pyropes at different temperatures and pressures. *Phys Chem Minerals* 29:362–368
- Volkov SYu, Grechushnikov BN, Sevastyanov BK, Tsvetkov VB (1981) A sapphire cold finger for getting intermediate temperatures. *Prib i tech Experimenta* 2:251–253 (in Russian)
- Yamanaka T, Takeuchi Y (1983) Ordering-disordering transition in  $\text{MgAl}_2\text{O}_4$  spinel at high temperature up to 1700°C. *Z Kristallogr* 165:65–78